

The Insula of Reil Revisited: Multiarchitectonic Organization in Macaque Monkeys

D. S. Gally¹, M. N. Gally^{1,4}, D. Jeanmonod², E. M. Rouiller³ and A. Morel¹

¹Center for Clinical Research and ²Department of Functional Neurosurgery, University Hospital Zürich, CH-8091 Zürich, Switzerland and ³Unit of Physiology and Program in Neurosciences, Department of Medicine, Faculty of Sciences, University of Fribourg, CH-1700 Fribourg, Switzerland

⁴Current address: Kantonsspital St. Gallen, Klinik für Neurochirurgie, CH-9007 St. Gallen, Switzerland

D. S. Gally and M. N. Gally have contributed equally to this work

Address correspondence to Dr Anne Morel, Center for Clinical Research, University Hospital Zürich, Sternwartstrasse 6, CH-8091 Zürich, Switzerland. Email: anne.morel@usz.ch.

The insula of Reil represents a large cortical territory buried in the depth of the lateral sulcus and subdivided into 3 major cytoarchitectonic domains: agranular, dysgranular, and granular. The present study aimed at reinvestigating the architectonic organization of the monkey's insula using multiple immunohistochemical stainings (parvalbumin, PV; nonphosphorylated neurofilament protein, with SMI-32; acetylcholinesterase, AChE) in addition to Nissl and myelin. According to changes in density and laminar distributions of the neurochemical markers, several zones were defined and related to 8 cytoarchitectonic subdivisions (Ia1–Ia2/I d1–I d3/Ig1–Ig2/G). Comparison of the different patterns of staining on unfolded maps of the insula revealed: 1) parallel ventral to dorsal gradients of increasing myelin, PV- and AChE-containing fibers in middle layers, and of SMI-32 pyramidal neurons in supragranular layers, with merging of dorsal and ventral high-density bands in posterior insula, 2) definition of an insula “proper” restricted to two-thirds of the “morphological” insula (as bounded by the limiting sulcus) and characterized most notably by lower PV, and 3) the insula proper is bordered along its dorsal, posterodorsal, and posteroventral margin by a strip of cortex extending beyond the limits of the morphological insula and continuous architectonically with frontoparietal and temporal opercular areas related to gustatory, somatosensory, and auditory modalities.

Keywords: immunohistochemical, mesocortex, parvalbumin, SMI-32, somatosensory

Introduction

The insula of Reil has gained much attention during the past decade owing to functional neuroimaging studies providing further evidence of its involvement in a wide range of functions, from sensory to visceral (Craig et al. 2000; Bamiou et al. 2003; Brooks et al. 2005; Kurth et al. 2010). The insula is part of a large mesocortical (paralimbic) domain with transitory architectonic characteristics between allo- and isocortex and a tripartite division into agranular (or periallocortical), dysgranular (or proisocortical), and granular (or isocortical) sectors (Ia, Id, and Ig, respectively) (Mesulam and Mufson 1982a). In contrast to other mesocortical regions, in particular the cingulate and orbitofrontal cortices (Hof and Nimchinsky 1992; Carmichael and Price 1994, 1995a, 1995b; Hof et al. 1995; Carmichael and Price 1996; Vogt et al. 2005), the anatomy of the insula has not, or only little, been reexplored since the seminal studies in the 1960s and 1980s (Roberts and Akert 1963; Mesulam and Mufson 1982a, 1982b; Mufson and Mesulam 1982, 1984; Mesulam and Mufson 1985), and these

earlier studies still serve as a basis for relating functional and connectivity studies in monkeys (Jones and Burton 1976; Friedman and Murray 1986; Friedman et al. 1986; Augustine 1996; Chikama et al. 1997; Saleem et al. 2008). The extent of the insula is generally depicted as bounded by the 2 limbs of the limiting sulcus, but anteriorly, beyond the limen insula, the uncertain border with orbitofrontal cortex lead Mesulam and Mufson (1982a) to place only an “arbitrary division” between the 2 areas. More recent studies on orbitofrontal cortex suggest several subdivisions within the agranular insula near its junction with the piriform cortex (Carmichael and Price 1994). Along the dorsal and posterior margin of the insula, several studies focusing on parietal opercular cortex suggest extension of somatosensory cortex into Ig, with several areas (SII, PV, PR, VS) identified physiologically and by connectivity with primary somatosensory cortex (Cusick et al. 1989; Krubitzer et al. 1995; Disbrow et al. 2003; Coq et al. 2004). These areas were included in a larger SII area in earlier studies (Jones and Burton 1976; Friedman et al. 1980; Robinson and Burton 1980b, 1980c; Juliano et al. 1983; Friedman et al. 1986). In contrast, a separate interoceptive, thermosensory area, distinct from parietal somatosensory cortex was proposed at the dorsal margin of the insula (Craig 1995), but a clear anatomical definition and localization of this region is still lacking. On the temporal opercular side, the boundary between the insula and belt auditory cortex, especially anteriorly, was not clearly defined (Morel et al. 1993; Hackett et al. 1998; Kaas and Hackett 2000), and the region was designated as parainsular area (Pi) in earlier studies (Jones and Burton 1976; Schneider et al. 1993).

The aim of the present study was to reappraise the anatomical organization of the insula and its boundaries with opercular areas in macaque monkey using a multiarchitectonic approach based on the distribution of the calcium-binding protein parvalbumin (PV), the nonphosphorylated neurofilament protein (with SMI-32), and acetylcholinesterase (AChE), in addition to Nissl and myelin stainings. The combination of these markers has been particularly relevant to define cortical and subcortical areas (Campbell and Morrison 1989; Jones and Hendry 1989; Del Rio and DeFelipe 1994; Jones et al. 1995) and their distribution in the insula should provide a new basis for relating functional (physiological) and connectional studies in monkeys. Preliminary results were presented in abstract form (Gally et al. 2009).

Materials and Methods

The brains of 10 adult rhesus (*Macaca mulatta*) and 3 cynomolgus (*Macaca fascicularis*) monkeys, used in previous experiments (Liu et al. 2002; Morel et al. 2005; Cappe et al. 2007, 2009), were reexamined for the present study (Supplementary Table 1). Most

material had already been processed with different staining procedures (Nissl, SMI-32, PV, AChE), and additional series of free-floating sections that have been stored at -20°C in a cryoprotectant solution were stained for myelin with the Gallyas (1979) method or for AChE to complete series that were not optimally stained for the cortex. In short, after perfusion with paraformaldehyde 4%, the brains were removed, blocked, and after cryoprotection, cut frozen in the coronal plane using a sliding cryotome or a cryostat. Several adjacent series of $50\ \mu\text{m}$ sections were collected in phosphate buffer (PB) and immediately mounted or stored at -20°C in a cryoprotectant solution for later processing. The different immunocytochemical procedures correspond to those published elsewhere (Liu et al. 2002; Morel et al. 2005) and are described in more details in Supplementary Material and Methods. For illustrations, photomicrographs were captured from a low-power Leica MZ16 microscope and digital camera (Leica DFC420). The files were then exported to Adobe Photoshop (version CS3) for contrast and brightness adjustments and imported in Adobe Illustrator (version CS4) software for production of the final montages.

Data Analysis

Delimitations of insular and adjacent cortical areas were plotted using a Leica (DM 6000 B) microscope equipped with a digital camera (MBF CX 9000) and a computerized plotting system (NeuroLucida, MicroBrightField, Inc., Williston, VT, USA). Every second or fourth section in each series was analyzed. The architectonic borders were assessed

independently by at least 2 investigators and most congruent borders were taken as reliable. The NeuroLucida plots containing partial section contours of the insular-opercular cortex and architectonic borders identified in Nissl, PV, SMI-32, AChE, and myelin series were exported as vector data to Adobe Illustrator.

Unfolded Maps

In order to compare architectonic organization obtained with different markers in a given monkey and evaluate the interindividual variability, a method was developed to graphically unfold the opercular and insular cortices. The unfolded maps of the insula were obtained by measuring the distances between the superior (slis) and inferior (ilis) limbs of the limiting sulcus, as well as between architectonic boundaries along layer 4 (or between layers 3 and 5 in absence of layer 4). These measurements were plotted for sections at regular intervals. To ease comparison between the different cases, each unfolded map was fitted with the fundus of the slis as reference. This reference was placed perpendicular to the tangent of the curve of the slis (Fig. 1, middle panel). Positions of architectonic borders were then plotted on vertical lines orthogonal to the axis of the slis (horizontal line, right panel, Fig. 1). Distances between sections were determined taking into account number of series and thickness ($50\ \mu\text{m}$) of sections and scaled to the map. Unfolded maps were generally reconstructed from sections at $800\ \mu\text{m}$ intervals, but smaller ($400\ \mu\text{m}$) or larger ($1600\ \mu\text{m}$) intervals

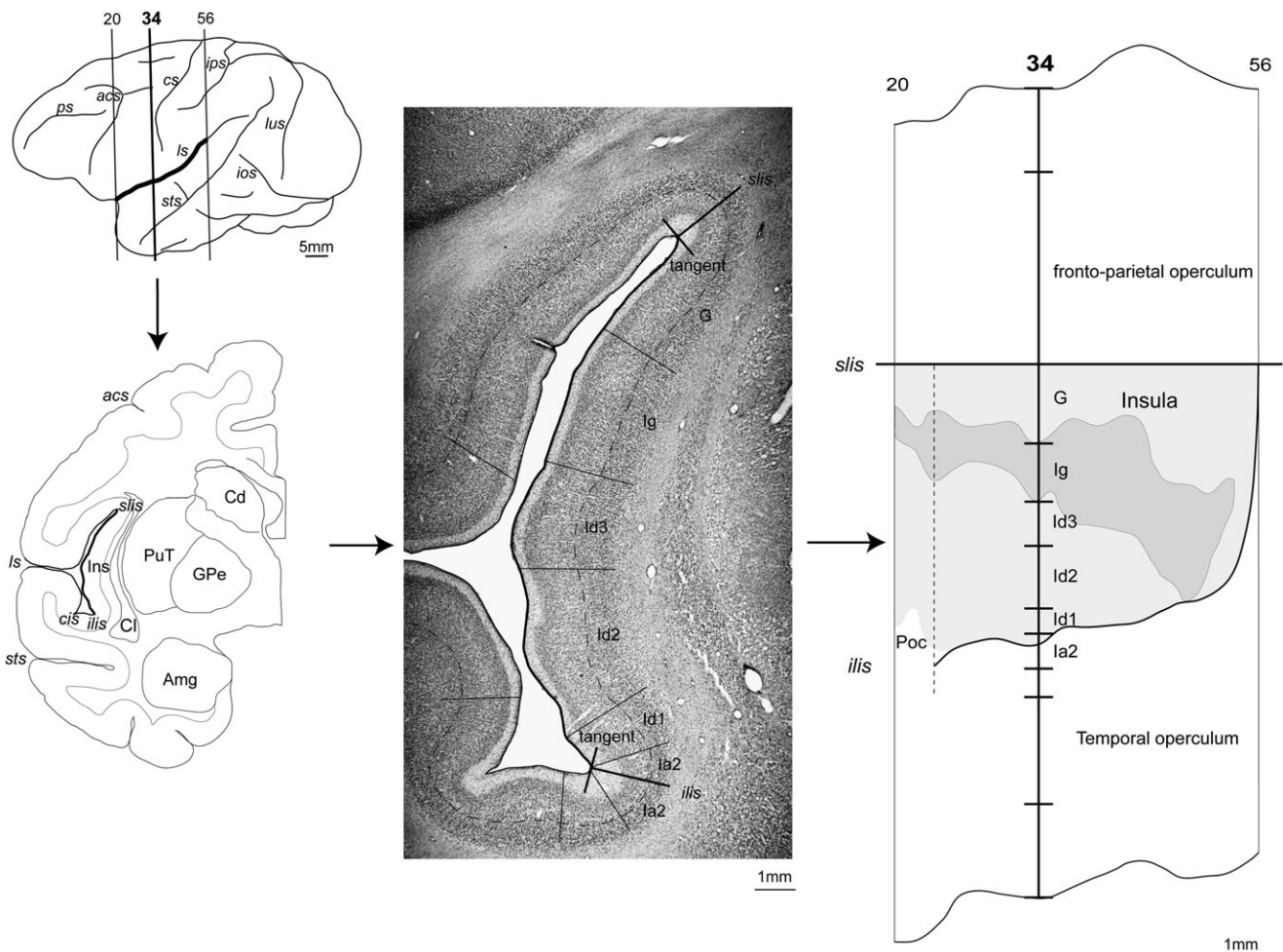


Figure 1. Diagram of the method used for unfolding the insula. For each frontal section (here illustrated for Nissl section 34 of monkey Mk4 in anterior half of the insula, left panels), the contour of layer IV (or between III and V) is traced on the scanned section and added to NeuroLucida plots of operculoinular contours and architectonic boundaries (dotted line in middle panel). The distances measured between slis and ilis (or slis and limit with Poc at the junction with orbitofrontal cortex) as well as between architectonic boundaries are projected onto a straight line, starting from slis as reference point. The resulting unfolded map is illustrated in right panel, and the surface of an insular domain (here the granular $lg = lg_1 + lg_2$) exemplified by a darker gray area. See Supplementary List of Abbreviations.

were also used in some cases to complete the map or when a section was missing, respectively. The area bounded by the 2 limbs of the limiting sulcus and anteriorly up to the limen of the insula (indicated by a vertical dotted line) is defined as the “morphological” insula. The method which is illustrated in Figure 1 has also the advantage of minimizing deformations resulting from mounting sections on slides, such as nonoptimal orientation of opercular or intrasulcal cortex, and facilitates comparisons between stainings and section levels with minimal bias since the morphological insula undergoes limited deformation. However, some series of sections, particularly those stained for myelin, suffered more shrinkage than others due to histological processing. As this shrinkage affects mainly distances measured after staining (i.e., in the plane of section) but not between sections (distances measured prior to sectioning, on brains undergoing similar fixation and cryoprotection procedures), no correction factor was added. Some additional minor errors may arise with the method, such as when tracing layer IV which is not visible in all stains or absent in agranular subdivisions. However, the source of this error, which is not quantifiable, is similar in all cases and thus can be considered negligible for the reconstructions and comparisons of the unfolded maps.

Variability Measurements

In order to compare architectonic organization with different markers and evaluate variability of the insula between monkeys, it was necessary to establish an area defined with similar criteria in all cases. To this purpose and because of uncertain border between orbitofrontal and insular Ia/Id, we selected the area delimited by the limiting sulcus up to the limen of the insula anteriorly (morphological insula). Interindividual variability of the insula was assessed by differences in morphology and/or sizes, as measured from Nissl maps (the least distorted by histological processing), in 3 monkeys (Fig. 4). The maps were superposed graphically using the sulcus and the anterior limit of the morphological insula (vertical dotted red line) as references for alignment. Boundaries of corresponding subdivisions defined in the 3 monkeys were selected and the variability range for each subdivision estimated by the surface between the most dorsal and the most ventral limits of the area selected. The same procedure was followed for the other subdivisions and an unfolded map of interindividual variability of insular subdivisions was obtained (lower right panel of Fig. 4).

Terminology

The terminology for the insular cortex follows the cytoarchitectonic parcellation into agranular, dysgranular, and granular sectors, with additional subdivisions as described in the Results. For opercular, perinsular areas, the nomenclature combines a classical terminology based mainly on cytoarchitectonic studies with more recent ones based on chemoarchitectonic, physiological, and/or connective maps in the somatosensory, auditory, and orbitofrontal opercular cortex (see Supplementary List of Abbreviations).

Results

Analysis of the neurochemical compartmentalization of the insula and adjoining cortex relied mostly on the distribution of PV, SMI-32, and AChE staining, exhibiting consistent patterns along the cortex. However, changes were often gradual and only reliable borders (recognized by at least 2 independent observers) were considered. In order to relate the present architectonic data to the classical subdivisions of the insula, similar cytoarchitectonic and myeloarchitectonic criteria as described by others were used for the delimitation. In one case (Mk12), an unfolded map was obtained for each staining (5 maps, Supplementary Fig. 3) and thus direct comparison was possible. Altogether, 3 maps for each staining were obtained from different monkeys. In one (Mk4, Fig. 7), an extended map illustrates the delimitation of frontoparietal and temporal opercular areas as identified on the basis of PV immunostaining

and by comparison with previous studies on somatosensory, auditory, and gustatory cortex.

The cyto- and immunohistochemical characteristics of the insular subdivisions are described in Table 1 and illustrated in Figure 2 with high-power photomicrographs taken at corresponding anteroposterior locations along the insula and ordered according to cytoarchitectonic subdivisions. An additional series of photomicrographs at the level of the primary somatosensory area 3b is presented for comparison. The insular multiarchitectonic subdivisions are also illustrated in composite low-power photomicrographs of frontal sections taken at regular anteroposterior intervals (Fig. 3). Like in Figure 2, the photomicrographs of Nissl, PV, and SMI-32 and those stained for myelin and AChE stand from 2 different monkeys (Mk4 and Mk13, respectively). In spite of differences in morphology between the 2 animals, the sections which were taken at similar anteroposterior levels of the insula exhibit changes that correspond to those observed in other monkeys. For myelin, AChE, PV, and SMI-32, the insula was subdivided into zones, numbered from 0 (or 1) to 5 (or 6) according to changes in density/intensity and laminar distribution of cellular or fiber staining (0 is the lowest) (see Figs 5 and 6; Supplementary Figs 1 and 2). The positions of borders are not necessarily coincident with those of Nissl, as discussed further below.

In all unfolded maps except one (SMI-32 for Mk8 in Fig. 6), the different architectonic subdivisions are depicted for the morphological insula and for a short distance anterior to the level of the limen (indicated by a vertical dotted line) (Figs 4–6; Supplementary Figs 1–3). Ventral extension beyond ilis is only represented in Nissl maps (Fig. 4) because of uncertainty related to these borders in other stainings, particularly at the level of the region termed parainsular (Pi, Fig. 7).

Cytoarchitecture

Nissl staining was analyzed in detail in 3 monkeys, and the boundaries were identified according to criteria described by others in agranular, dysgranular, and granular domains. According to the presence of granule cells in layers II and IV, the thickness of these layers, and the sublamination of III and V, we recognized 8 subdivisions within the insula (see Table 1): 2 agranular (Ia1 and Ia2), 3 dysgranular (Id1–Id3), 2 granular (Ig1 and Ig2), and a hypergranular “G” subdivision which also extends into parietofrontal and temporal opercula. The term hypergranular is used here to depict a laminar pattern close to that seen in primary sensory areas but less pronounced particularly in terms of layer IV thickness (see Fig. 2). Sequential numbering in each cytoarchitectonic domain corresponds to progressively more differentiated cortex, in particular with the appearance and increasing thickness of granular layers II and IV. In most parts of the insula, however, changes were only gradual and no sharp borders could be detected. The most obvious changes were between Ig and G, characterized by marked increase in the thickness of layer IV, sublamination of layers III and V, as well as between Ia2 and Id1 with the appearance, even subtle, of granular cells in layers II and IV, and sublamination of layer V (Fig. 2 and Table 1).

On unfolded maps (Fig. 4), the ventral limit of cytoarchitectonic subdivisions is shown beyond the limits of the ilis, especially in the middle portion of the insula. Whether these extensions should still be considered as part of the insula

Table 1
Multiarchitectonic characteristics of insular subdivisions

	Nissl	PV	SMI-32	AChE	Myelin
G	Similar to Ig2 but with broader and denser layer IV	High density of fibers in layers II–V, most prominent in middle layers (deep III and IV)	Increase number of stained neurons in layer III compared with Ig1–Ig2	Moderate to high fiber staining in layers I, III/IV, and deep V; lighter and more diffuse staining in others	Increase of density of myelinated fibers up to layer III and lighter plexuses in II; clear outer BB
Ig2	Moderate change from Ig1, mainly increase of layer IV thickness and more conspicuous sublamination of III and V	Overall similar pattern as in Ig1	Overall similar pattern as in Ig1	Overall similar pattern as in Ig1	Slight increase of myelinated fibers in deep layer III and clear outer BB
Ig1	Increase of layers II and IV thickness and clear separation V/VI	Increase of neuropil staining in layers II–V, particularly in layer IV and deep III	Same density of staining in layer V as in Id3 but noticeable increase of stained cells in layer III	Increase in layers III and IV, with clear separation from layer deep V	Similar to Id3 but with clear outer BB (separated by lighter myelin in V)
Id3	Thickening of layer IV	Similar pattern as in Id2 but with moderate fiber staining extending also in layer II	Strong staining in layer V (dendrites and few somata) and increase in layer III, with clear separation by unstained layer IV	Slight increase of neuropil staining in layer III and separation with the darker band in upper V	Thickening of fiber plexuses in layers IV–VI and progressive appearance of an outer BB
Id2	Layer II well developed and clearly distinct from III; thin but clear layer IV; sublamination layer V	Marked fiber staining in layer IV and gradual increase in layer III	Appearance of few cells in layer III; strong dendritic staining and few cells in layer V	Similar pattern as in Id but with intensification of fiber staining in layer IV and deep layer III	Densification of radial fibers in layers IV and V but no distinct outer BB
Id1	Irregular and thin layer II; faint granular layer IV; and separation V–VI	Narrow band of fiber staining in layer IV and more diffuse in deep III and V	Intense dendritic staining in layer V; nearly absent in superficial layers	Dense staining in layers I and V/VI, very light in II and III, and progressive increase in layer IV	Generally weak myelin, except for thick plexuses in layer VI
Ia2	Appearance of a patchy layer II and no granular layer IV; barely visible separation V–VI	Generally low fiber staining. Only moderate staining in layer V	Low fiber staining and rare cells in fused layers II/III	Densification of fiber staining in superficial layers I and fused II/III	Similar pattern to Ia1; slightly lower density of myelinated fibers in fused layers V/VI
Ia1	Fused layers II–III and V–VI; no granular layers II and IV	Fiber staining in fused layers II/III and only faint in V/VI	Diffuse neuropil staining and few cells in fused layers II/III; very faint in layers V/VI	Intense fiber staining in fused layers II/III and V/VI	Fine fiber plexuses parallel to cortical surface in layer I and deep layers V/VI

cannot be determined at the present time and were included in the broadly defined parainsular area (Pi, Fig. 7).

Myeloarchitecture

The myelin stain with the Gallyas method was applied in 3 cases (Supplementary Table 1) and in one monkey (Mk12, Supplementary Fig. 3) it could be compared with adjacent series stained for PV, SMI-32, and AChE, in addition to Nissl. In this and other immunohistochemical stainings, the term “zone” is used to make the distinction with Nissl “subdivisions.” The pattern of intracortical myelin in the insula shows a progressive increase of the density of fibers toward cortical surface, with appearance of a clear outer band of Baillarger (BB) in zones 5 and 6 (Table 1 and Figs 2 and 3; Supplementary Fig. 1). The extension of vertical fibers into more superficial layers (including layer II) observed in zone 6 is in continuity with the pattern seen in dorsal and posterior parietal opercular areas. Not only the density but also the general orientation of fibers changed, from more or less parallel to cortical surface in anteroventral insula (zones 1–2, corresponding to agranular and first dysgranular field, Id1) to vertically oriented from zones 3 to 6 (Figs 2 and 3; Supplementary Fig. 1). Zone 1 is also characterized by relatively dense fiber plexuses in superficial layers and oriented parallel to cortical surface. Zones labeled 3 β and 4 β designate similar overall intensity of cortical myelin as in zones 3 and 4 but with somewhat different

patterns across layers, such as clearer outer BB in zone 4 β than in zone 4.

Acetylcholinesterase

The distribution of AChE fibers was analyzed in 7 monkeys (Supplementary Table 1), and unfolded maps were obtained for 3 of them (Supplementary Fig. 2). Several zones were labeled 1–6, from a low to high density gradient of AChE containing fibers. To take into account differences in laminar distribution (but overall similar intensities of staining), zones 3–5 in anterior insula were differentiated from zones 3 β to 5 β in middle and posterior insula. The most intense staining was observed in fiber plexuses in layer I and in deep layers in the most ventral and anterior part of the insula (corresponding to agranular cortex) (Table 1 and Figs 2 and 3, and zone 6 in Supplementary Figs 1 and 2). Progressing more dorsally and posteriorly, the intensity of AChE increased in layer III in continuity with the patterns observed in parietal opercular cortex. However, in contrast to the patterns seen with the cyto- and myeloarchitecture (as well as with PV and SMI-32), there is a reversal of the gradient in anterior insula, with a circumscribed domain of low intensity AChE staining (zones 1 and 2) more dorsally (Figs 2 and 3; Supplementary Fig. 2). This particular pattern seen in all cases is mostly due to the area of very strong AChE staining in deep layers in the

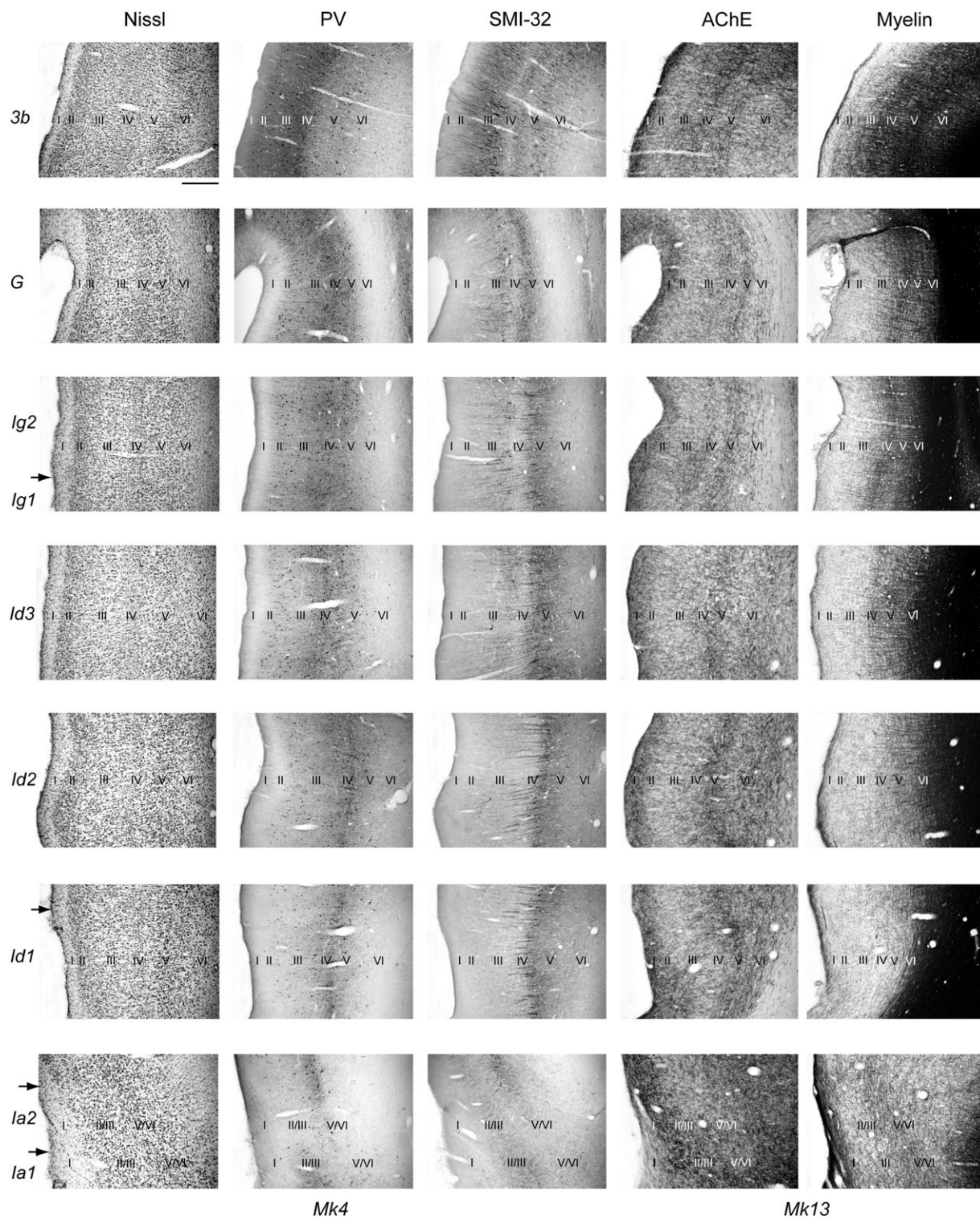


Figure 2. Multiarchitectonic characteristics of insular subdivisions. High-power photomicrographs of Nissl, PV, and SMI-32 (adjacent sections from Mk4) and myelin and AChE stainings (adjacent sections from Mk13, taken as close as possible to the levels of sections shown for Mk4) are ordered according to cytoarchitectonic subdivisions (G to Ia1, from top to bottom) and reoriented parallel to the cortical surface. The upper row shows multiarchitectonic characteristics in primary somatosensory area 3b for comparison. In each row, positions of cortical layers identified on Nissl sections are projected onto the other photomicrographs taking into account differences in shrinkage due to the different staining procedures. Corresponding architectonic criteria are described in Table 1. Scale bar (upper left photomicrograph): 500 μ m.

anteroventral insula characterized by zone 6. In middle insula, the relatively low AChE seen at level of Id near the ilis, extends into Pi, while increasing again toward core auditory cortex in the lower bank of the lateral sulcus (see Supplementary Fig. 2).

Parvalbumin

The pattern of immunostaining for PV is illustrated by microphotographs in Table 1 and in Figures 2 and 3, as well as on unfolded maps in Figures 5 and 7. PV immunoreactivity

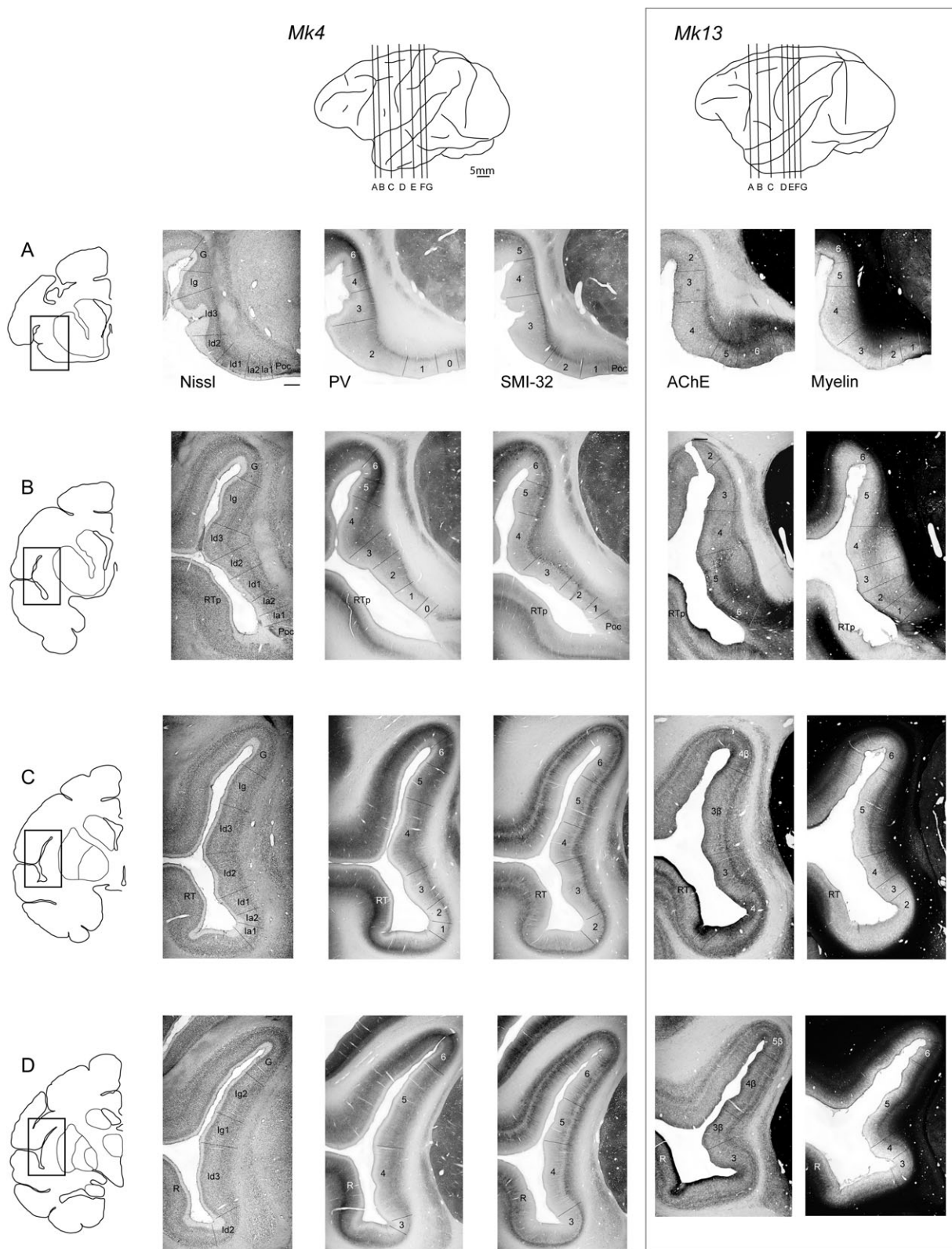


Figure 3. Composite photomicrographs of Nissl, PV, SMI-32, AChE, and myelin stainings at different frontal levels of the insula in Mk4 and Mk13. Positions of Nissl sections (A–G) are indicated on lateral views of the left hemisphere of each monkey (top drawings) and the area enclosed by the photomicrographs indicated by a rectangle on drawings of the corresponding frontal sections (left column). The architectonic boundaries are shown for all stainings and correspond to those depicted in Figure 5 and Supplementary Figures 1 and 2 for PV, myelin, and AChE, respectively, in relation to their corresponding unfolded maps. Auditory areas AI, R, RT, and RTp in temporal operculum are also indicated for guidance. Notice the differences in morphological aspects of the insula between Mk4 and Mk13 (particularly at middle level, bottom row). However, the gradients seen with AChE and myelin follow closely those observed for Nissl, PV, and SMI-32. Scale bar (upper left photomicrograph): 1 mm.

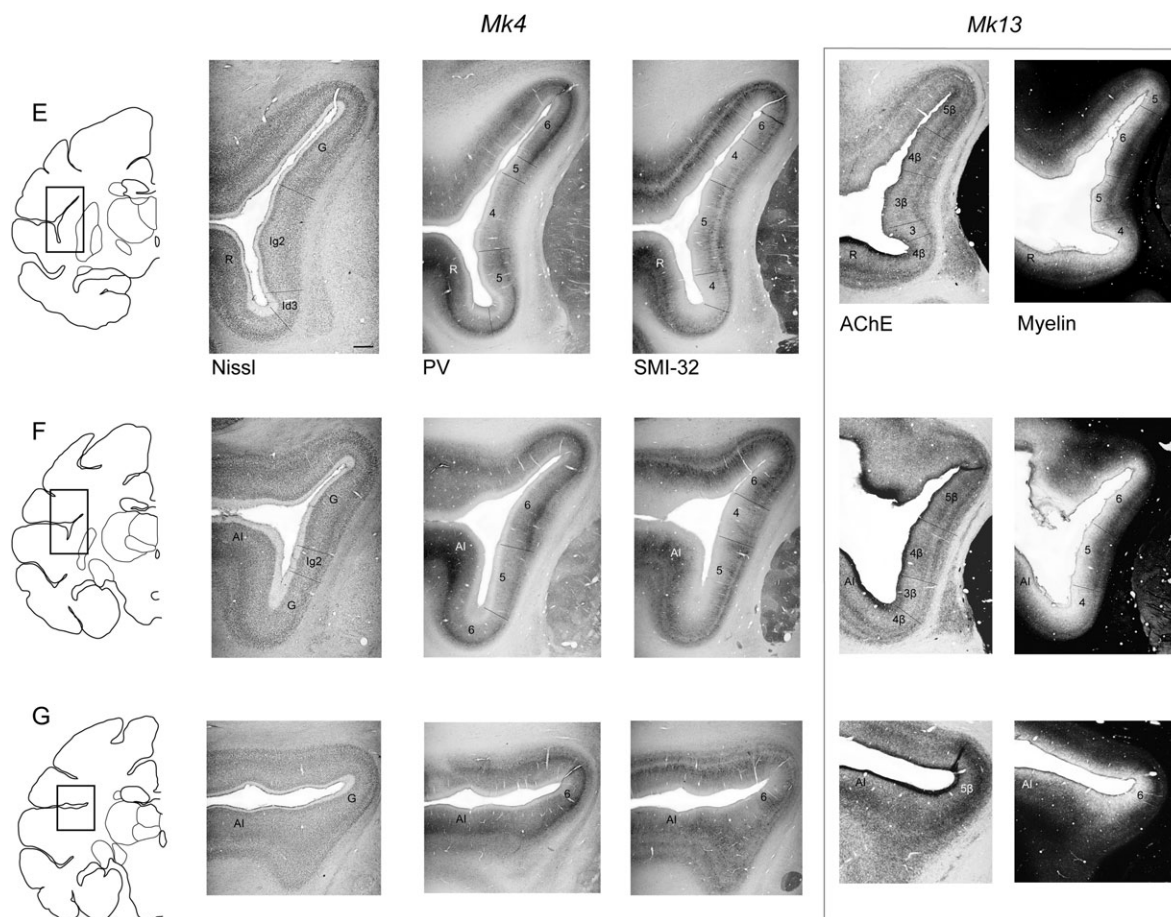


Fig. 3. Continued.

is present in both cells and fiber plexuses. The changes along the insula and adjoining cortex are particularly marked with fiber staining but there are also changes in the laminar distribution and density of labeled neurons, as shown in Figure 2. We focused mainly on fiber staining (as also described in Table 1) with the highest density in layer IV and deep layer III along the dorsal and posterior margin of the insula (zones 5 and 6) as well as in frontoparietal and posterior temporal opercular cortex. Toward the ventral and anterior insula, the PV immunostaining decreases progressively in middle layers across dysgranular subdivisions Id3 to Id1 (Figs 2, 3, and 5), to become nearly absent in agranular field Ia2. Near the Poc, in Ia1, PV expression increases again in fused layers II/III (with only rare cells) (Fig. 2), the 2 subareas were included in one zone (zone 0). Similar patterns were observed for the 3 monkeys illustrated in Figure 5.

SMI-32

The gradient of SMI-32 immunostaining is most pronounced in a ventral to dorsal and posterior direction by the increase of the density of pyramidal neurons in layer III (and to some extent also layer V) (zones 5 and 6, Figs 2, 3, and 6; see also Table 1). Parallel to the gradient seen with stained neuronal somata and process, a progressive increase of a more diffuse and fine neuropil staining is observed in layer V (Fig. 2). This gradient extends beyond the sulcus into frontoparietal opercular cortex and onto the lateral surface, with the strongest density of layer III neurons in primary areas 3b (Table 1 and Fig. 2). A similar

very dense layer III immunostaining was also seen in the temporal opercular cortex, in AI, while decreasing clearly in areas R and RT, as well as in medial and caudal belt areas (Fig. 6). In the anteroventral insula, the number of SMI-32 cells and the intensity of neuropil staining in layer V decreased progressively in dysgranular domains Id1/Id2 (zone 2) to become very light in agranular field Ia2 (Figs 2 and 3). An increase again of neuropil staining in fused layers II/III characterizes Ia1, in a similar pattern to that of PV immunostaining.

Unfolded Maps of the Insula: Variations in Size

Unfolded maps of each staining are presented for 3 different monkeys in Figures 4 and 5 and Supplementary Figures 1 and 2, and comparison between different stainings shown for one monkey in Supplementary Figure 3. Overall, the extension of the insula in the anteroposterior axis appears relatively constant (between 16.5 and 17.5 mm) when measured along the lateral sulcus on a lateral view of the hemisphere (e.g., in Fig. 1). Because of variable distances and uncertainty for the insular/orbitofrontal boundary, the anteroposterior extent of the morphological insula represents a more accurate value for comparing the different maps. The values which range between 12 and 14.4 mm (average 13.4 mm) were not corrected for shrinkage and thus do not reflect "in vivo" dimensions. Measurements along the plane of sections (mediolateral, i.e., along the short axis of the insula) vary more than in the other directions, and this is due to distortion (shrinkage)

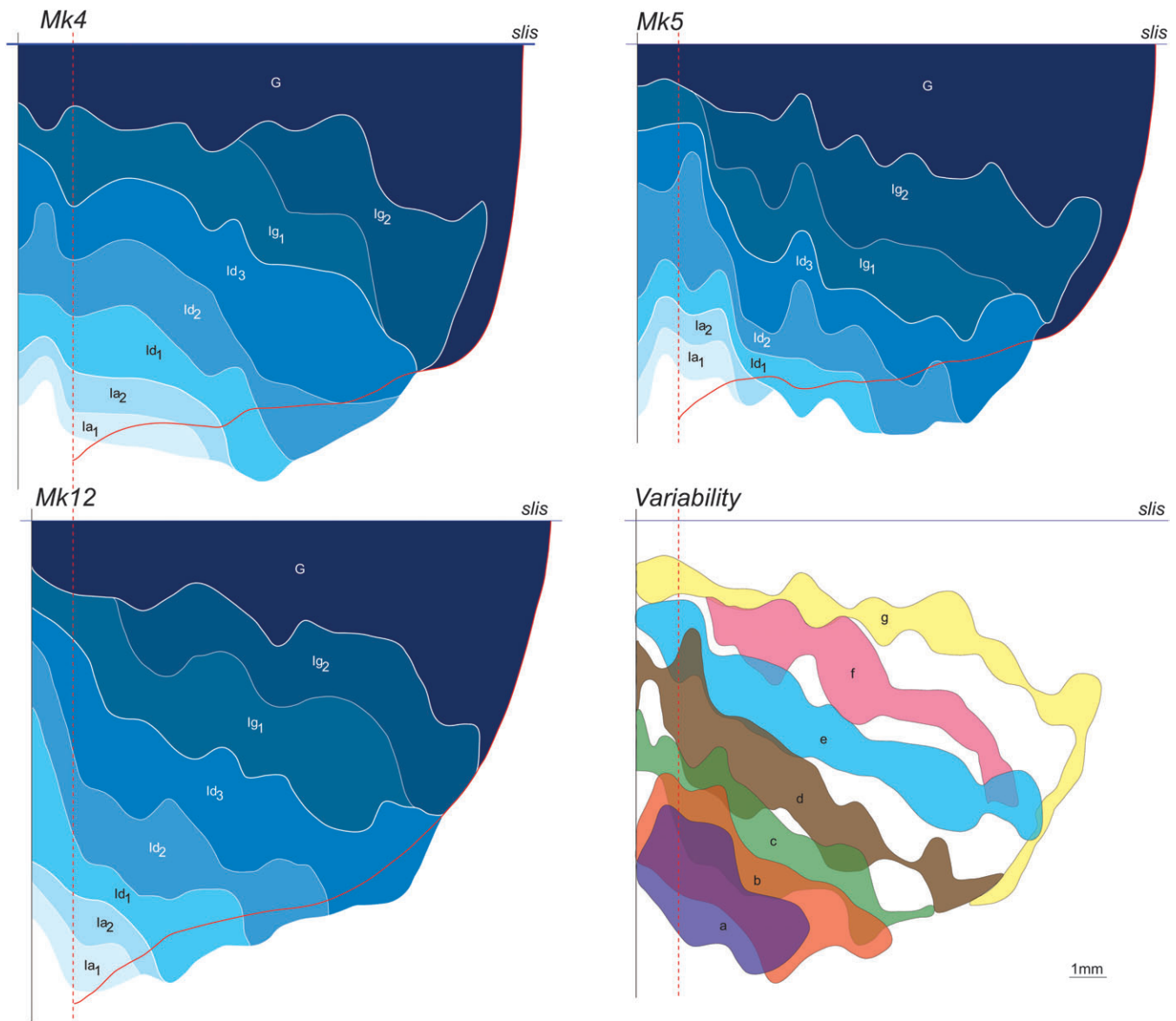


Figure 4. Unfolded maps of cytoarchitectonic subdivisions in 3 monkeys (maps Mk4, Mk5, and Mk12) and their interindividual variability. In each individual map, the vertical dashed red line indicates the anterior limit (limen) of the "morphological" insula, the horizontal straight red line, the limit of slis, and the curved red line, the limit of the ilis. The graph in lower right panel represents interindividual variability of the different cytoarchitectonic subdivisions, with "a" corresponding to Ia1-Ia2; "b" to Ia-Ia2; "c" to Id1-Id2; "d" to Id2-Id3; "e" to Id-Ig; "f" to Ig1-Ig2; and "g" to Ig-G borders.

factors that differ between histological processings (e.g., shorter mediolateral dimensions for the maps based on myelin stain; Supplementary Figs 1 and 3) but also differences in insular morphology. For example, the maximum mediolateral extent of the morphological insula tends to be larger on Nissl than on myelin maps, but the interindividual variability is of the same magnitude for both (11–14 and 10–13 mm, respectively).

Multiarchitectonic Organization: Comparison between Cytoarchitectonic and Immunohistochemical Subdivisions

Similar patterns and orientation of insular subdivisions were observed in all stainings, with low-to-high, anteroventral to dorsal and posterior gradients of immunohistochemical staining (zones 0 or 1–6) in parallel to cytoarchitectonic progression from agranular (Ia) to hypergranular (G) fields. The

main exception is the AChE staining, where 2 zones of high density of fiber staining (zones 4–6 and 4 β –5 β ; Supplementary Fig. 2) border anteroventral and posteriorly zones of lower density (zones 1–3 and 3 β). The distribution of AChE fibers across cortical layers, that is, from deep layers anteroventral to both supra- and infragranular distributions posteriorly, however, follows a gradient in the same overall orientation as in the other maps. One particular feature of the architectonic organization seen with PV, SMI-32, and AChE is the merging in posterior insula of the dorsal zone of enhanced staining with an equally dense area extending from the temporal operculum. Together they surround a strip of lower intensity, particularly conspicuous with PV immunostaining (zone 4 interspersed between zones 5 and 6). This pattern is consistent across monkeys (see Figs 5 and 6 and Supplementary Fig. 2) and differs from Nissl and myelin gradients which do not exhibit such obvious reversals (see Fig. 4

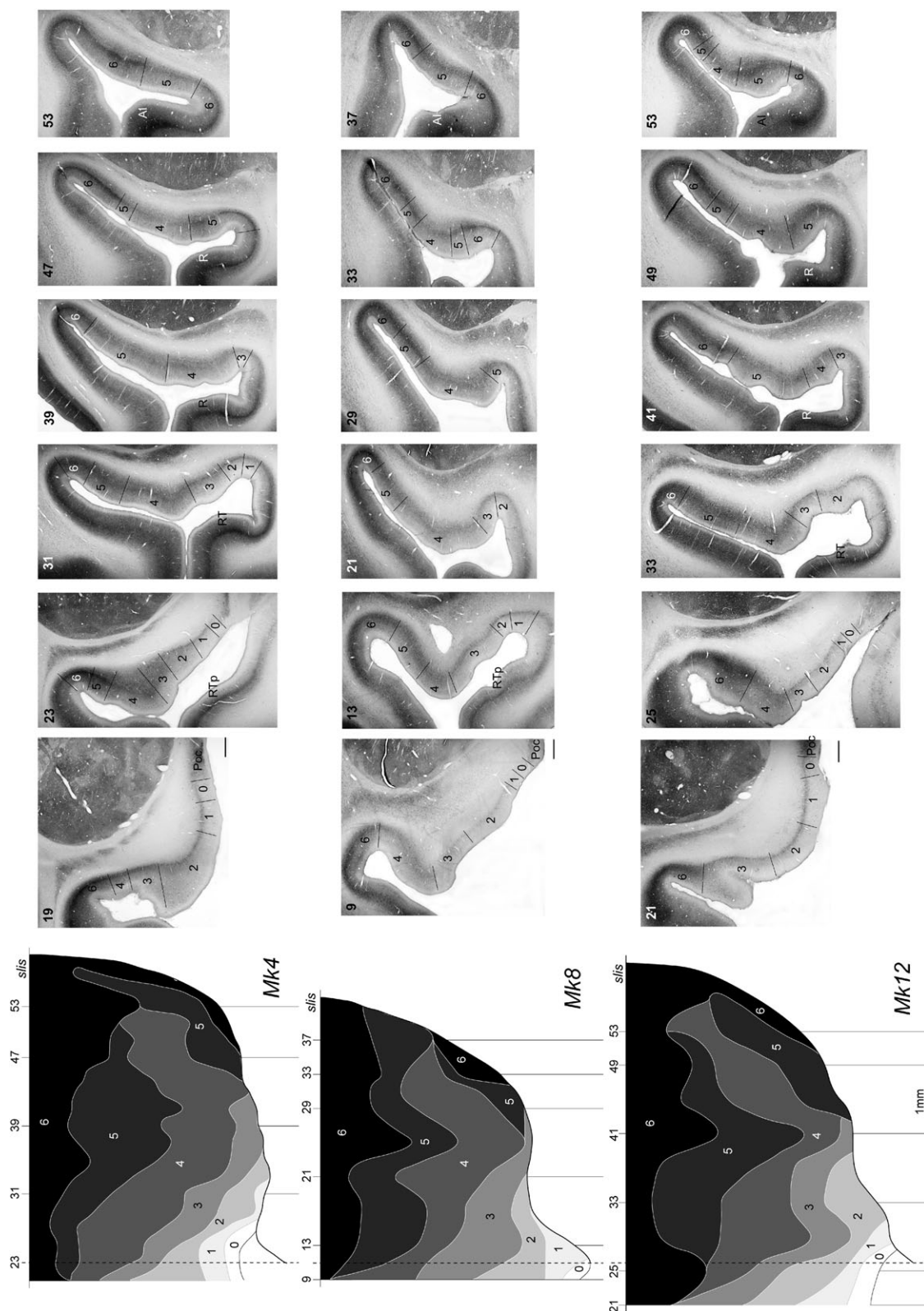


Figure 5. Unfolded maps of PV immunostaining (left panels) and corresponding series of photomicrographs of frontal sections in 3 monkeys (Mk4, Mk8, and Mk12). The levels of sections are indicated in the corresponding maps. For Mk4 (upper row), levels of section represented in the unfolded map and that illustrated by the most anterior photomicrograph (S19) differ by 0.8 mm, but the patterns of PV immunostaining are quite similar. Because of differences in size, intervals (absolute values) between sections are not necessarily equivalent in the 3 monkeys but were chosen to correspond best to similar anteroposterior levels of the insula. Series from Mk4 are also illustrated in Figure 3 (levels A–G) for comparisons with the other patterns of staining. Zones 0–6 correspond to gradients of increasing density of PV immunostaining in fiber plexuses, most notably in middle layers (deep III and IV). For other conventions, see Figures 3 and 4. Scale bars (left photomicrographs): 1 mm.

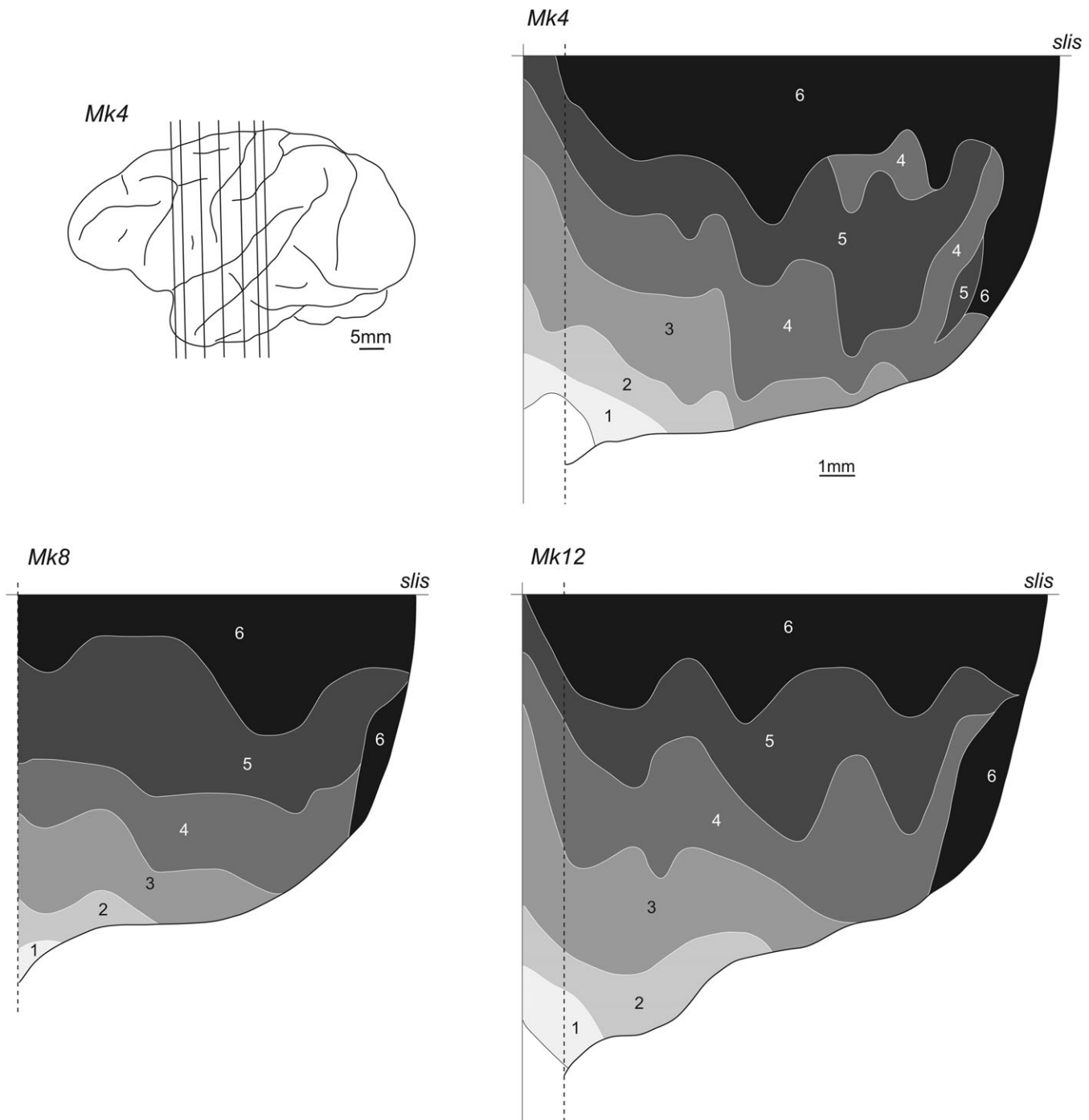


Figure 6. Unfolded maps of SMI-32 in 3 monkeys (same cases as in Fig. 5). Zones 1–6 correspond to increasing density of immunostained pyramidal cells in layers III and V. The same series of sections are also illustrated in Figure 3 (levels A–G) for comparisons with other patterns of staining. For other conventions, see Figures 3 and 4.

and Supplementary Fig. 1). The difference appears in the upward posterior tail of variability zone “e” in the upper left diagram of Supplementary Figure 3 depicting variability of the limits of insular subdivisions defined by different stainings in comparison to cytoarchitectonic subdivisions.

Extended Map of the Insula and Opercular Areas

In several monkeys, multiarchitectonic boundaries were also plotted beyond the limits of the morphological insula, that is, into frontoparietal and temporal opercula (e.g., in Fig. 1). In one

case (Mk4, Fig. 7), delimitations of opercular areas and their relations to insular subdivisions on the basis of fiber immunostaining for PV are presented on an extended unfolded map. The patterns are also illustrated on frontal sections of the left hemisphere (left panels in Fig. 7). According to the high density of PV immunostained fiber plexuses in middle layers along the dorsal, posterior, and posteroventral margin of the morphological insula (zone 6), as well as the continuity with areas of similar intensity in opercular cortex, we propose the term insula “proper” for the territory encompassing zones 0–5 (see

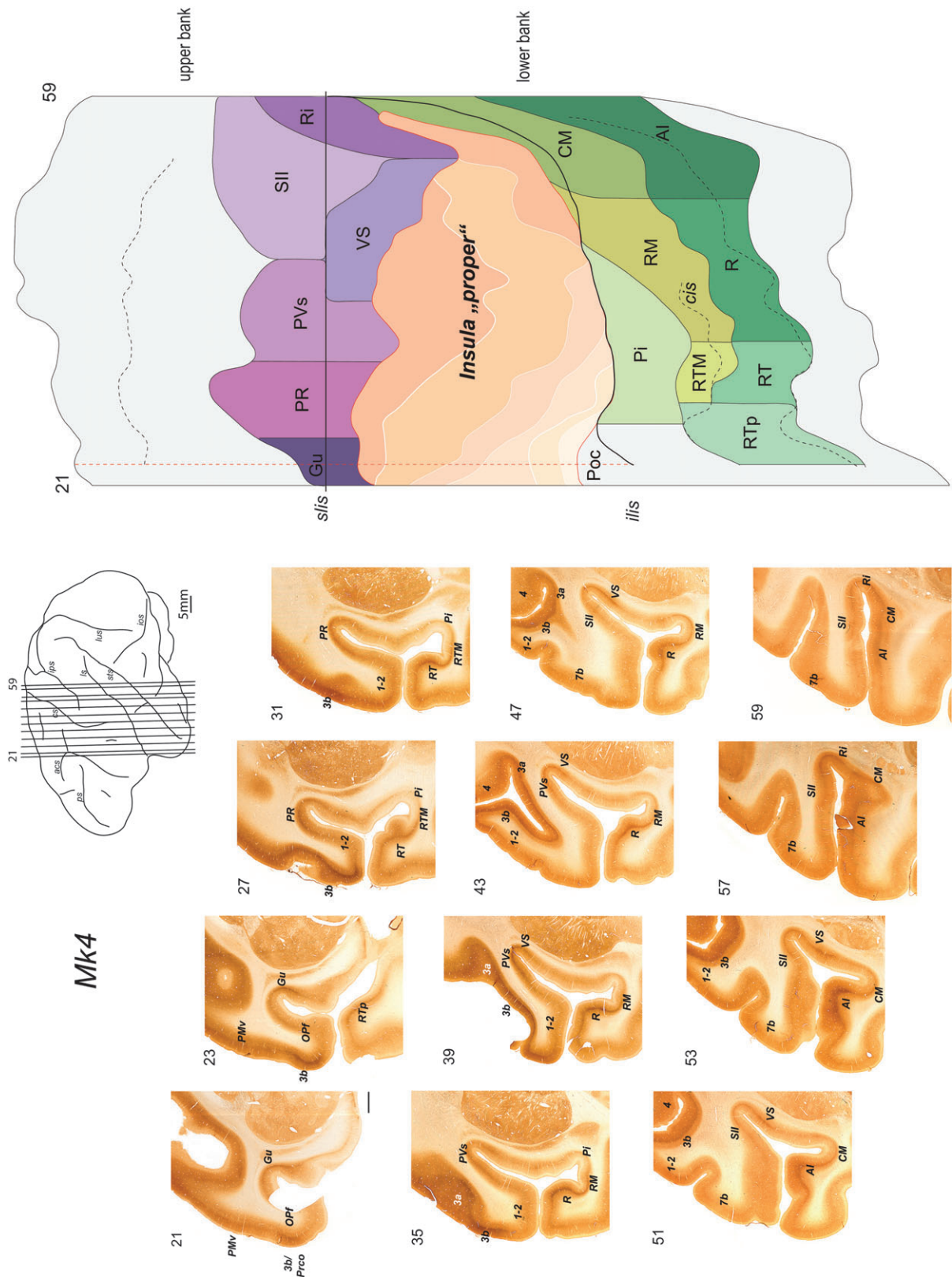


Figure 7. Insular and opercular areas delimited by PV immunostaining in monkey Mk4. Series of scanned images of frontal sections are ordered from anterior to posterior, from 21 to 59 (left panels) and the corresponding unfolded map of the lateral sulcus illustrated in right panel. Several cortical areas outside the insula “proper” (enclosing zones 0–5) were relatively well identified according to previous architectonic studies (e.g., 3b, AI, R, RT, CM, RM, Gu), while others (e.g., PVs, PR, VS, RTp) are less well defined and their positions assumed on the basis of physiological mapping and/or connective studies. In the temporal opercular cortex, only areas medial to the “core” auditory cortex (medial belt) are labeled on the sections and on the unfolded map. The intermediate area between rostromedial belt (RTM and RM) and the “morphological” insula is termed parainsular (Pi) to follow earlier studies of the temporal opercular cortex. See Supplementary List of Abbreviations. Scale bar (upper left photomicrograph): 2 mm.

also Fig. 5). A similar territory can be delimited on the basis of SMI-32 immunostaining (zones 1-5, Fig. 6), while only the posterior half of the insula may correspond to part of the insula proper on the basis of AChE (Supplementary Fig. 2).

The terminology and approximate boundaries proposed for opercular areas depicted in PV immunostained frontal sections and on the extended unfolded map stem from others' studies on orbitofrontal (gustatory), parietal (somatosensory), and temporal (auditory) cortex (see Discussion).

Discussion

The major findings on the multiarchitectonic organization of the monkey's insula are the following: 1) the presence of several additional subdivisions within the major cytoarchitectonic domains (Ia, Id, and Ig), 2) definition of an insula proper with distinct immunohistochemical patterns from the rest of the morphological insula, and 3) intrusion of orbitofrontal gustatory, parietal somatosensory, and temporal auditory cortical areas into the dorsal, ventral, and posterior morphological insula.

Multiarchitectonic Organization: Relation to Classical Ia, Id, and Ig Domains

The number of cytoarchitectonic subdivisions (up to 8) encompassing the morphological insula was related to structural changes that were gradual rather than abrupt. However, these changes, although subtle, were reliably detected by different observers in all cases. The most confident boundaries were between cytoarchitectonic G and Ig (or Ig2) and between Ia2 and Id1, whereas more tenuously defined within a given domain (e.g., between Ig1 and Ig2 or Id2 and Id3). In order to compare with previously defined Ia, Id, and Ig subdivisions in the same primate species, surface areas were measured graphically and the proportions given in percentages of the morphological insula (see unfolded maps and histograms in Fig. 8). Despite the approximation for the surfaces measured and the position of the anterior limit of the morphological insula in the former representations (Mesulam and Mufson 1982a, 1985; Friedman and Murray 1986; Friedman et al. 1986), the values are indicative of overall variations of these insular domains across studies. The most distinct features are 1) the small proportions of the G hypergranular field (less than 10%) in previous studies compared with about one-third in the present report, 2) differences in granular and dysgranular fields representations in previous studies, with nearly inverted proportions of Ig and Id but equal proportions in the present one, and 3) overall, small area devoted to agranular domain. The differences between the 3 maps reflect the difficulty of setting boundaries in mesocortex with transitory architectonic characteristics (Mesulam and Mufson 1982a; Mesulam 2000) and explain the variability in the borders and number of subdivisions proposed in other mesocortical areas. Additional factors, such as multiarchitectonic comparisons in the present work and connectivity patterns in others, may influence the placement of borders, although these should be considered as negligible. Interestingly, a displacement of the dysgranular field more anteriorly, with concomitant increase of granular field in macaque monkey compared with squirrel monkey, was mentioned by Jones and Burton (1976). This tendency is particularly noticeable in our maps with the large portion devoted to granular fields (~65% for Ig + G). Whether it finds

correlates along primate evolution, including man, cannot be answered at the present time.

The comparison between cytoarchitectonic and neurochemical divisions based on immunohistochemical staining for PV, SMI-32, and AChE provides information pertinent to the functional organization of the insula: 1) The differential distribution of PV fiber immunostaining, particularly in middle layers, is most likely related to the patterns of thalamic projections to the insula and adjacent opercular areas, 2) The progression of SMI-32 pyramidal neurons from deep layers (V/VI) in agranular insula to increasing numbers in layer III in dysgranular and granular sectors is associated with different types of corticocortical connections as observed in several other cortical areas (Hof et al. 1995), and 3) The gradient of high-to-low AChE fibers in anterior insula corresponds to that of cortical AChE-containing fibers described by others, that is, densest in periallocortical and progressively declining toward granular fields in all mesocortical areas in monkey (Mesulam and Mufson 1982a; Mesulam et al. 1984; Mesulam 2000). The reversal depicted in the posterior (granular) insula in our maps is related to specific increase of AChE fiber density in supragranular layers, more than to overall change across cortex, and this parallels other neurochemical gradients, including the relatively large G field in Nissl maps.

The Relation of the Insula to Opercular Areas and Definition of an Insula Proper

In the cytoarchitectonic division of the insula, we distinguished between a hypergranular G subdivision and granular insula (Ig1-Ig2) on the basis of clear thickening of layer IV, sublamination of layers III and V, and well-demarcated layer VI (Table 1). This strip of cortex which continues beyond the limits of the morphological insula into frontoparietal and posterior temporal opercula, corresponds largely to zones of densest PV in middle layers, of SMI-32 neurons in layer III, and AChE fibers in layers III and IV, as well as dark myelin and clear outer BB. Relatively few investigations directly addressed the functional organization of the insula, but physiological and connectivity studies in opercular areas provide clues to support the functional interpretation of an insula proper as defined by multiarchitectonic criteria. These aspects are discussed in relation to others' views on the functional role and organization of the insula, in particular at its dorsal margin with the parietal operculum.

In anterior insula, at the junction with orbitofrontal cortex, the dorsal PV-enhanced region is similar to that described by Carmichael and Price (1994) and identified as gustatory area. The same region is known to receive thalamic projections from the VPMpc nucleus (Roberts and Akert 1963; Pritchard et al. 1986). The densest projections from this gustatory thalamic nucleus are restricted to a small area at the fundus of slis anterior to the border of insular-opercular cortex, intercalated between dysgranular insular (Id) and opercular (OPd) areas (e.g., Fig. 2; Pritchard et al. 1986). This represents presumably the primary gustatory cortex, but additional gustatory areas have been proposed in granular and dysgranular insula (de Araujo and Simon 2009), and one could correspond to the zone of lower PV immunostaining on adjacent dysgranular field (Figs 5 and 7, present study; Carmichael and Price 1994). In our extended map of opercular areas, we designated the most anterior PV enhanced area as gustatory (Gu), but it is possible that part of PR may also represent gustatory modality.

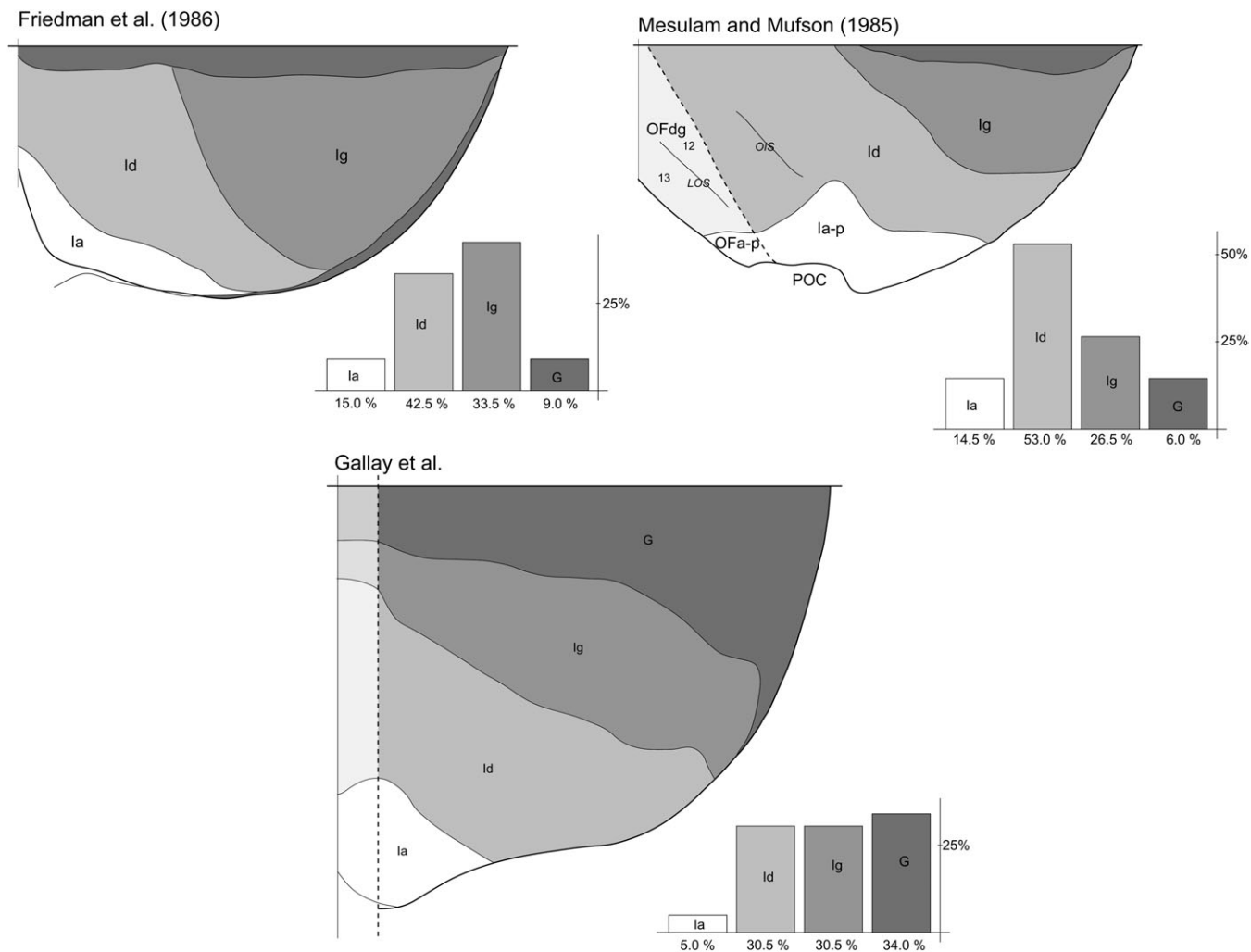


Figure 8. Comparison of cytoarchitectonic divisions of the insula in earlier studies (Mesulam and Mufson 1985; Friedman et al. 1986) and in the current study (Gallay et al.). The unfolded maps were all fitted with the fundus of the sulci and the surface of each insular subdivisions measured in mm² using a special Adobe Illustrator (version CS4) plug-in ("path area"). The relative proportion of each subdivision was then calculated in percent of the total surface of the "morphological" insula. The current map (Gallay et al.) is a graphical mean of the variation of the limits of the different Nissl subdivisions (regrouped in la, ld, and lg) in 3 monkeys (Mk4, Mk5, and Mk12). It is important to note that unfolded maps obtained for earlier studies were adapted from diagrammatic representations of "exploded or planar" maps but even if the sizes differ, we consider that the proportions given for each major subdivision, though approximate, are suitable values for comparison with our data.

The functional interpretation of the middle dorsal and posterior margin of the morphological insula and its relation to parietal opercular areas is still subject to controversial views. One the one hand, Craig (1995) designated part of the dorsal insula as cortical target of lamina I spinothalamic tract (STT) via thalamocortical projections from the so-called VMpo nucleus. However, this area is only poorly defined anatomically and its localization most probably overlaps with field G and the area of enhanced PV, SMI-32, AChE, and dense myelination extending into parietal opercular cortex in our maps. More recently, STT projections to insular cortex were clearly confined to Ig (as also defined cytoarchitectonically in the present study) (Dum et al. 2009). On the other hand, recent studies devoted to opercular somatosensory areas, suggest extension of the ventral somatosensory area (VS) and the parietal rostral area (PR) into the morphological insula, particularly in prosimian and New World monkeys (Krubitzer et al. 1995; Qi et al. 2002; Disbrow et al. 2003; Wu and Kaas 2003; Coq et al. 2004). These areas were first included into a larger SII in previous studies (Roberts and Akert 1963; Jones and Burton 1976; Friedman

et al. 1980, 1986; Robinson and Burton 1980b, 1980c; Juliano et al. 1983; Friedman and Murray 1986; Schneider et al. 1993). The boundaries of parietal opercular areas represented in the unfolded map of Figure 7 are proposed on the basis of PV immunostaining, but their correspondence with the different somatosensory maps remains to be confirmed, in particular for PR which is defined mainly by its connectivity with PV and SII (Qi et al. 2002; Disbrow et al. 2003).

The extension of PV, SMI-32, and AChE enhanced immunohistochemical staining into posterior and ventral temporal operculum is consistent with architectonic and mapping studies of the primate auditory cortex, in particular with the boundaries proposed for medial and posterior belt areas (Morel et al. 1993; Hackett et al. 1998; Jones 2003). These are represented together with core auditory areas in the superior temporal plane in Figure 7. If limits between core and medial belt cortex are relatively clear, those between medial belt and the insula are less well defined and their boundaries relative to morphological landmarks (e.g., circular and limiting sulci) may differ. For example, area RM is generally confined to the ventral

bank of LS, while extending into the insula in other reports (Morel et al. 1993). Whether this corresponds to relatively high PV immunostaining in the posteroventral part of the insula proper has to be confirmed. The limits between anterior medial belt and the insula have not been well defined and the area was designated by parainsular (Pi) as in earlier studies (Jones and Burton 1976; Schneider et al. 1993).

The multiarchitectonic definition of an insula proper restricted to about two-third of the morphological insula is also supported by functional and connectivity data. In spite of the limited physiological investigations of the insula, there is clear evidence for somatosensory representation in the posterior granular field (Ig), although with differences of receptive field properties (very large, often including the whole body), absence of clear topographic organization, and less responsiveness to passive stimulation than in adjacent opercular areas (Robinson and Burton 1980a, 1980c; Schneider et al. 1993; Burton et al. 1995). Very much attention has been paid in recent years to the involvement of the operculoinsular cortex in pain processing, particularly with neuroimaging in humans (Peyron et al. 2002; Brooks et al. 2005), but little is known about the organization of nociceptive neurons in monkeys. Auditory responses were also reported in the posterior insula or near the border with somatosensory VS area, possibly overlapping partially with the insula proper (Coq et al. 2004; Remedios et al. 2009). How other modalities/functions are represented by neurons or neuronal arrays in the monkey insula awaits further investigations.

Relations to Subcortical and Cortical Connections

Connectivity studies provide important information on the functional organization of the insula. Major investigations of the thalamic and cortical connections of different insular domains were conducted few decades ago and the patterns related to somewhat different cortical and thalamic parcellations (Roberts and Akert 1963; Jones and Burton 1976; Mesulam and Mufson 1982b; Mufson and Mesulam 1984; Friedman and Murray 1986; Friedman et al. 1986; Carmichael and Price 1995b). Thalamic projections arise from several nuclei, but these tend to be organized in the insula, such that projections from the posterior complex (SG, Po) and ventral posterior inferior (VPI) are directed at the posterior granular insula, and that of the parvocellular VPMpc (or VMB) directed at more anterior areas, including the agranular insula. The latter nucleus is also considered as principal thalamic afferent to taste areas(s) in the orbitoinsular cortex (Pritchard et al. 1986). Additional nuclei contribute to the thalamic projections to the insula and their targets support functional differences, such as only Ia appears to receive inputs from limbic midline and mediodorsal (magnocellular part, MDmc) nuclei (Friedman and Murray 1986). The pattern of thalamocortical connections is consistent, at least to some extent, with the gradients of PV immunostaining observed in the present study. Indeed, a close relation between PV rich fiber plexuses in layers IV and deep layer III and afferents from PV dominant thalamic nuclei has been demonstrated, particularly in the auditory system (Jones 2003). Thus, the very dense PV immunostaining in area 3b and AI/R also shown in the present study reflects prominent thalamic input from PV-rich VPL and ventral medial geniculate (MGv) neurons, respectively. The relatively moderate PV immunostaining in the insula proper is consistent with

projections from nonprimary, associative nuclei such as the posterior complex (SG-Li, Po) containing fewer PV neurons (and conversely, more calbindin positive cells). In this context, it is difficult to reconcile the projections from the so-called VMpo (corresponding to SG/Po) to the dorsal margin of the insula characterized by dense PV fiber staining in middle layers.

Projections to the striatum also support the present multiarchitectonic organization of the insula, with a gradient of projections from Ig to dorsolateral (sensorimotor), Id to central ventral striatum, and Ia to the accumbens nucleus (limbic part) (Chikama et al. 1997).

Relatively few studies have directly addressed cortical projections to (or from) the insula with injections localized in the different subdivisions. These studies, together with complementary data from tracer injections in other cortical territories (sensory, paralimbic, limbic) (Mesulam and Mufson 1982b; Mufson and Mesulam 1982; Friedman et al. 1986; Augustine 1996), reveal some specificity related to insular architectonic boundaries. The representation of sensory (somatosensory/auditory) in posterior and of visceral/autonomic functions in anterior insula, conforms to the general granular to agranular gradient along the insula, as well as to immunohistochemical changes observed in the insula proper. The laminar distributions of cortical projecting neurons (from and to different sectors of the insula) (Friedman et al. 1986) bear some relationship with the laminar gradients of pyramidal SMI-32 neurons. In agranular insula, these were confined to deep layers (V/VI), while in dysgranular and granular, were distributed in both III and V, with progressive increase in layer III toward hypergranular field G. This gradient within the insula can also be related to predictive model of laminar distributions of cortical projections from agranular/dysgranular neurons (deep layers) to granular (or eulaminate) areas and also to intermediate positions according to “hierarchical levels” (e.g., increase of SMI-32 in supragranular layers in Id compared with Ia) (Barbas and Rempel-Clower 1997).

Conclusions

The present multiarchitectonic organization of the insula provides a framework for future investigations on the functional (electrophysiological) and connective aspects of the insula in primates, as well as for comparative studies in different primate species, including humans. A more thorough neuroanatomical exploration of the human insula will be particularly important to support localization of structural (MRI, DTI) and functional (fMRI) imaging data that significantly improved in spatial resolution. A first step toward this aim has been reported recently by a study focused on the posterior human insula (Kurth et al. 2009).

Supplementary Material

Supplementary material can be found at: <http://www.cercor.oxfordjournals.org/>

Funding

Swiss National Science Foundation (grants 31-054178.98, 32-118175 to A.M. and 110005, 132465 to E.M.R.).

Notes

The authors are particularly indebted to V. Moret, V. Streit, and A. Baechler for histological processing. Special thanks also to J. Liu and A. Poveda for their assistance in some parts of the experiments and/or histological processing and to H. Job for help in photographic montages. *Conflict of Interest*: None declared.

References

- Augustine JR. 1996. Circuitry and functional aspects of the insular lobe in primates including humans. *Brain Res Rev.* 22:229-244.
- Bamiou DE, Musiek FE, Luxon LM. 2003. The insula (Island of Reil) and its role in auditory processing. Literature review. *Brain Res Rev.* 42:143-154.
- Barbas H, Rempel-Clover N. 1997. Cortical structure predicts the pattern of corticocortical connections. *Cereb Cortex.* 7:635-646.
- Brooks JC, Zambreanu L, Godinez A, Craig AD, Tracey I. 2005. Somatotopic organisation of the human insula to painful heat studied with high resolution functional imaging. *Neuroimage.* 27:201-209.
- Burton H, Fabri M, Alloway K. 1995. Cortical areas within the lateral sulcus connected to cutaneous representations in areas 3b and 1: a revised interpretation of the second somatosensory area in macaque monkeys. *J Comp Neurol.* 355:539-562.
- Campbell MJ, Morrison JH. 1989. Monoclonal antibody to neurofilament protein (SMI-32) labels a subpopulation of pyramidal neurons in the human and monkey neocortex. *J Comp Neurol.* 282:191-205.
- Cappe C, Morel A, Barone P, Rouiller EM. 2009. The thalamocortical projection systems in primate: an anatomical support for multisensory and sensorimotor interplay. *Cereb Cortex.* 19:2025-2037.
- Cappe C, Morel A, Rouiller EM. 2007. Thalamocortical and the dual pattern of corticothalamic projections of the posterior parietal cortex in macaque monkeys. *Neuroscience.* 146:1371-1387.
- Carmichael ST, Price JL. 1994. Architectonic subdivision of the orbital and medial prefrontal cortex in the macaque monkey. *J Comp Neurol.* 346:366-402.
- Carmichael ST, Price JL. 1995a. Sensory and premotor connections of the orbital and medial prefrontal cortex of macaque monkeys. *J Comp Neurol.* 363:642-664.
- Carmichael ST, Price JL. 1995b. Limbic connections of the orbital and medial prefrontal cortex in macaque monkeys. *J Comp Neurol.* 363:615-641.
- Carmichael ST, Price JL. 1996. Connectional networks within the orbital and medial prefrontal cortex of macaque monkeys. *J Comp Neurol.* 371:179-207.
- Chikama M, McFarland NR, Amaral DG, Haber SN. 1997. Insular cortical projections to functional regions of the striatum correlate with cortical cytoarchitectonic organization in the primate. *J Neurosci.* 17:9686-9705.
- Coq JO, Qi H, Collins CE, Kaas JH. 2004. Anatomical and functional organization of somatosensory areas of the lateral fissure of the New World titi monkey (*Callicebus moloch*). *J Comp Neurol.* 476:363-387.
- Craig A. 1995. Spinal projections of lamina I neurons. In: Besson JM, Guilbaud G, Ollat H, editors. Forebrain areas involved in pain processing. Paris: John Libbey Eurotext. p. 13-26.
- Craig AD, Chen K, Bandy D, Reiman EM. 2000. Thermosensory activation of insular cortex. *Nat Neurosci.* 3:184-190.
- Cusick CG, Wall JT, Felleman DJ, Kaas JH. 1989. Somatotopic organization of the lateral sulcus of owl monkeys: area 3b, S-II, and a ventral somatosensory area. *J Comp Neurol.* 282:169-190.
- de Araujo IE, Simon SA. 2009. The gustatory cortex and multisensory integration. *Int J Obes (Lond).* 33(Suppl 2):S34-S43.
- Del Rio MR, DeFelipe J. 1994. A study of SMI 32-stained pyramidal cells, parvalbumin-immunoreactive chandelier cells, and presumptive thalamocortical axons in the human temporal neocortex. *J Comp Neurol.* 342:389-408.
- Disbrow E, Litinas E, Recanzone GH, Padberg J, Krubitzer L. 2003. Cortical connections of the second somatosensory area and the parietal ventral area in macaque monkeys. *J Comp Neurol.* 462:382-399.
- Dum RP, Levinthal DJ, Strick PL. 2009. The spinothalamic system targets motor and sensory areas in the cerebral cortex of monkeys. *J Neurosci.* 29:14223-14235.
- Friedman DP, Jones EG, Burton H. 1980. Representation pattern in the second somatic sensory area of the monkey cerebral cortex. *J Comp Neurol.* 192:21-41.
- Friedman DP, Murray EA. 1986. Thalamic connectivity of the second somatosensory area and neighboring somatosensory fields of the lateral sulcus of the macaque. *J Comp Neurol.* 252:348-373.
- Friedman DP, Murray EA, O'Neill JB, Mishkin M. 1986. Cortical connections of the somatosensory fields of the lateral sulcus of macaques: evidence for a corticolimbic pathway for touch. *J Comp Neurol.* 252:323-347.
- Gallay M, Gallay D, Poveda A, Rouiller E, Jeanmonod D, Morel A. 2009. The insula of Reil: multiarchitectonic organization in macaque monkeys and preliminary observations in humans. Program Nr 464.11/DD3. Neuroscience Abstract. Chicago (IL): Society for Neuroscience. Online.
- Gallyas F. 1979. Silver staining of myelin by means of physical development. *Neurol Res.* 1:203-209.
- Hackett TA, Stepniewska I, Kaas JH. 1998. Subdivisions of auditory cortex and ipsilateral cortical connections of the parabelt auditory cortex in macaque monkeys. *J Comp Neurol.* 394:475-495.
- Hof PR, Nimchinsky EA. 1992. Regional distribution of neurofilament and calcium-binding proteins in the cingulate cortex of the macaque monkey. *Cereb Cortex.* 2:456-467.
- Hof PR, Nimchinsky EA, Morrison JH. 1995. Neurochemical phenotype of corticocortical connections in the macaque monkey: quantitative analysis of a subset of neurofilament protein-immunoreactive projection neurons in frontal, parietal, temporal, and cingulate cortices. *J Comp Neurol.* 362:109-133.
- Jones EG. 2003. Chemically defined parallel pathways in the monkey auditory system. *Ann N Y Acad Sci.* 999:218-233.
- Jones EG, Burton H. 1976. Areal differences in the laminar distribution of thalamic afferents in cortical fields of the insular, parietal and temporal regions of primates. *J Comp Neurol.* 168:197-247.
- Jones EG, Dell'Anna ME, Molinari M, Rausell E, Hashikawa T. 1995. Subdivisions of macaque monkey auditory cortex revealed by calcium-binding protein immunoreactivity. *J Comp Neurol.* 362:153-170.
- Jones EG, Hendry SH. 1989. Differential calcium binding protein immunoreactivity distinguishes classes of relay neurons in monkey thalamic nuclei. *Eur J Neurosci.* 1:222-246.
- Juliano SL, Hand PJ, Whitsel BL. 1983. Patterns of metabolic activity in cytoarchitectural area SII and surrounding cortical fields of the monkey. *J Neurophysiol.* 50:961-980.
- Kaas JH, Hackett TA. 2000. Subdivisions of auditory cortex and processing streams in primates. *Proc Natl Acad Sci U S A.* 97:11793-11799.
- Krubitzer L, Clarey J, Tweedale R, Elston G, Calford M. 1995. A redefinition of somatosensory areas in the lateral sulcus of macaque monkeys. *J Neurosci.* 15:3821-3839.
- Kurth F, Eickhoff SB, Schleicher A, Hoemke L, Zilles K, Amunts K. 2009. Cytoarchitecture and probabilistic maps of the human posterior insular cortex. *Cereb Cortex.* 20:1448-1461.
- Kurth F, Zilles K, Fox PT, Laird AR, Eickhoff SB. 2010. A link between the systems: functional differentiation and integration within the human insula revealed by meta-analysis. *Brain Struct Funct.* 214:519-534.
- Liu J, Morel A, Wannier T, Rouiller EM. 2002. Origins of callosal projections to the supplementary motor area (SMA): a direct comparison between pre-SMA and SMA-proper in macaque monkeys. *J Comp Neurol.* 443:71-85.
- Mesulam MM. 2000. Principles of behavioral and cognitive neurology. 2nd ed. Oxford: Oxford University Press.
- Mesulam MM, Mufson EJ. 1982a. Insula of the old world monkey. I. Architectonics in the insulo-orbito-temporal component of the paralimbic brain. *J Comp Neurol.* 212:1-22.
- Mesulam MM, Mufson EJ. 1982b. Insula of the old world monkey. III: efferent cortical output and comments on function. *J Comp Neurol.* 212:38-52.
- Mesulam MM, Mufson EJ. 1985. The insula of Reil in man and monkey. Architectonics, connectivity, and function. In: Peters A, Jones EG,

- editors. Cerebral cortex. New York: Plenum Publishing Corporation. p. 179-224.
- Mesulam MM, Rosen AD, Mufson EJ. 1984. Regional variations in cortical cholinergic innervation: chemoarchitectonics of acetylcholinesterase-containing fibers in the macaque brain. *Brain Res.* 311:245-258.
- Morel A, Garraghty PE, Kaas JH. 1993. Tonal organization, architectonic fields, and connections of auditory cortex in macaque monkeys. *J Comp Neurol.* 335:437-459.
- Morel A, Liu J, Wannier T, Jeanmonod D, Rouiller EM. 2005. Divergence and convergence of thalamocortical projections to premotor and supplementary motor cortex: a multiple tracing study in the macaque monkey. *Eur J Neurosci.* 21:1007-1029.
- Mufson EJ, Mesulam MM. 1982. Insula of the old world monkey. II: afferent cortical input and comments on the claustrum. *J Comp Neurol.* 212:23-37.
- Mufson EJ, Mesulam MM. 1984. Thalamic connections of the insula in the rhesus monkey and comments on the paralimbic connectivity of the medial pulvinar nucleus. *J Comp Neurol.* 227:109-120.
- Peyron R, Frot M, Schneider F, Garcia-Larrea L, Mertens P, Barral FG, Sindou M, Laurent B, Mauguier F. 2002. Role of operculoinsular cortices in human pain processing: converging evidence from PET, fMRI, dipole modeling, and intracerebral recordings of evoked potentials. *Neuroimage.* 17:1336-1346.
- Pritchard TC, Hamilton RB, Morse JR, Norgren R. 1986. Projections of thalamic gustatory and lingual areas in the monkey, *Macaca fascicularis*. *J Comp Neurol.* 244:213-228.
- Qi H, Lyon DC, Kaas JH. 2002. Cortical and thalamic connections of the parietal ventral somatosensory area in marmoset monkeys (*Callithrix jacchus*). *J Comp Neurol.* 443:168-182.
- Remedios R, Logothetis NK, Kayser C. 2009. An auditory region in the primate insular cortex responding preferentially to vocal communication sounds. *J Neurosci.* 29:1034-1045.
- Roberts TS, Akert K. 1963. Insular and opercular cortex and its thalamic projection in *Macaca mulatta*. *Schweiz Arch Neurol Neurochir Psychiatr.* 92:1-43.
- Robinson CJ, Burton H. 1980a. Organization of somatosensory receptive fields in cortical areas 7b, retroinsula, postauditory and granular insula of *M. fascicularis*. *J Comp Neurol.* 192:69-92.
- Robinson CJ, Burton H. 1980b. Somatotopographic organization in the second somatosensory area of *M. fascicularis*. *J Comp Neurol.* 192:43-67.
- Robinson CJ, Burton H. 1980c. Somatic submodality distribution within the second somatosensory (SII), 7b, retroinsular, postauditory, and granular insular cortical areas of *M. fascicularis*. *J Comp Neurol.* 192:93-108.
- Saleem KS, Kondo H, Price JL. 2008. Complementary circuits connecting the orbital and medial prefrontal networks with the temporal, insular, and opercular cortex in the macaque monkey. *J Comp Neurol.* 506:659-693.
- Schneider RJ, Friedman DP, Mishkin M. 1993. A modality-specific somatosensory area within the insula of the rhesus monkey. *Brain Res.* 621:116-120.
- Vogt BA, Vogt L, Farber NB, Bush G. 2005. Architecture and neurocytology of monkey cingulate gyrus. *J Comp Neurol.* 485:218-239.
- Wu CWH, Kaas JH. 2003. Somatosensory cortex of prosimian galagos: physiological recording, cytoarchitecture, and corticocortical connections of anterior parietal cortex and cortex of the lateral sulcus. *J Comp Neurol.* 457:263-292.